separations

MDPI

Article

Filter Modified with Hydrophilic and Oleophobic Coating for Efficient and Affordable Oil/Water Separation

Hunter Ross [1], Huyen Nguyen [1], Brian Nguyen [1], Ashton Foster [1], James Salud [1], Mike Patino [1], Yong X. Gan [2] and Mingheng Li [1,*]

[1] Department of Chemical and Materials Engineering, California State Polytechnic University, Pomona, CA 91768, USA
[2] Department of Mechanical Engineering, California State Polytechnic University, Pomona, CA 91768, USA
* Correspondence: minghengli@cpp.edu; Tel.: +1-909-869-3668

Abstract: To mitigate the damage of oil spills, a filter modified with a hydrophilic and oleophobic coating is proposed for affordable and efficient oil separation and recovery from water. The sol–gel method was chosen to produce a colloidal suspension of titanium dioxide particles for its ease of production and its versatility in application for many different substrates, including paper and cloth fabric. After immersing the substrates into a titanium-containing solution, three techniques were applied to increase the production of titanium dioxide—microwave-assisted, refrigeration, and ultra-sonication. Contact angle tests were done to investigate the change in the filter's oleophobicity. The titanium dioxide present on the surface of the filter was amorphous, but all treatment methods showed an improvement in oleophobicity. All treated filters improved oil filtration performance by up to eighty percent. The filters isolated motor oil from a mixture while allowing water to pass through. The coated filters also displayed photocatalytic activity by degrading methylene blue on its surface when exposed to sunlight, demonstrating the filter's self-cleaning ability. For real-world applications, the filter can be supported by a stainless mesh for enhanced strength and durability. While being dragged through the water, the filter collects the surface oil, allowing water to pass through via gravity.

Keywords: titanium dioxide; filter; oil spills; oil/water separation; sol–gel; hydrophilic and oleophobic coating

Citation: Ross, H.; Nguyen, H.; Nguyen, B.; Foster, A.; Salud, J.; Patino, M.; Gan, Y.X.; Li, M. Filter Modified with Hydrophilic and Oleophobic Coating for Efficient and Affordable Oil/Water Separation. *Separations* **2022**, *9*, 269. https://doi.org/10.3390/separations9100269

Academic Editor: Paraskevas D. Tzanavaras

Received: 23 August 2022
Accepted: 14 September 2022
Published: 28 September 2022

1. Introduction

Oil spills have severely impacted the ecological health of marine life and devastated coastlines. A recent example is the Huntington Beach Oil Spill that was detected in October 2021. The leakage, caused by a split in an underwater pipeline, spilled over 100,000 gallons of crude oil into coastal waters. Oil spills have become an environmentally critical issue because of their long-lasting consequences for the marine ecosystem and human health [1].

Traditional oil cleanup methods have poor oil recovery, slow operations, and pose the risk of introducing additional pollutants into the water [2]. In-situ burning is a technique that entails controlled burning of crude oil on the surface of the water. This produces harmful carbon emissions and can leave behind burnt oil residue. Burning requires optimal weather conditions, mild winds, and calm waves to maintain the controlled burn and minimize risk to humans and wildlife [2]. Another method, known as dispersion, involves airplanes spraying chemical dispersants that break down oil accumulating on the ocean surface into smaller droplets. While this method helps wildlife on the water's surface, the dispersants negatively impact marine wildlife. Skimming utilizes booms to enclose and collect oil. Skimmers collect the oil–water mixture into a recovery tank where gallons of oil and water are removed from spill location [3].

To overcome the shortcomings of these conventional methods, we propose trough-shaped filters modified by a unique hydrophilic and oleophobic coating for affordable

and efficient oil collection. As a result of these distinctive properties of the coating, the filter attracts polar water molecules while repelling the nonpolar oil molecules. The filters can be made of natural or synthetic materials (e.g., cotton, polyester, and polyamide) and supported by stainless steel mesh for enhanced strength and durability. When being pulled through water, the filters collect the surface oil while allowing water to pass through. The purpose of the filter developed in this work is to provide a preliminary result, leading to the development of a highly reproducible and easy to implement oil/seawater filter.

The development of surface materials that are both oleophobic and hydrophilic dates back to 2000, when Nakajima et al. [4] reported that, after 48 h UV illumination, the polycrystalline titania (TiO_2) thin film surface could have a larger hexadecane contact angle (25°) than water contact angle (0°). This discovery has generated immense interest in both academia and industry [5]. In recent years, this special coating has shown great potential for separating oil from water [6–8]. Moreover, the surface morphological structure can amplify the surface properties [9–11]. For example, incorporating nanostructures in the TiO_2 coating can make it hydrophilic and oleophobic, thus enhancing the absorption of water while improving the surface resistance to oil. Thereby, these TiO_2-based surface modifications can improve the efficiency of the oil/water separating filter.

Following the Huntington Beach Oil Spill, this project focused on creating a coated filter that can be implemented into machinery used to clean up oil spills. To accomplish this, TiO_2 was used as a coating material for natural fiber filters. The coated filters can potentially improve the speed of the cleanup efforts and oil recovery while remaining cost-effective and environmentally safe. Particularly, the coated filter can recover the spilled oil instead of burning the oil in the in situ burning and does not require a specific weather condition [2]. This method can be implemented to collect the spilled oil without any environmental and human health impacts compared to dispersion or in situ burning [12,13].

The photocatalytic properties of TiO_2 refer to its ability as a semiconductor to produce a powerful oxidizing hydroxyl radical when exposed to UV irradiation, oxygen, and water [14]. The hydroxyl can subsequently decompose organic molecules on its surface, often referred to as self-cleaning ability [14,15]. In the application of oil/water separation, wetted filters can be left to dry in the sun, exposing them to UV radiation oxygen and water cleaning on the filter surface.

TiO_2 will exhibit hydrophobic or hydrophilic behavior, depending on its crystal phase composition. In the study of crystal phase composition of TiO_2 and its effect on wettability, Vrakatseli et al. concluded that hydrophilicity is achieved with a rich anatase phase composition, while a rich rutile phase would make a filter become hydrophobic. Films consisting of high concentration of anatase phase exhibited strong hydrophilicity [16]. They concluded that anatase films retain hydrophilicity due to the donor–acceptor interaction between Ti-OH and water. In a study of the effect of TiO_2 coatings on rock surfaces, Hosseini et al. found significant anatase phase TiO_2 on hydrophilic and oleophobic surfaces [17]. For that reason, traditionally, the anatase phase would be favored for application concerning TiO_2 coatings. TiO_2 is ideal and applicable for use as a coating for an oil/water separating filter. The production of anatase phase TiO_2 typically requires heat treatment, as even low-temperature novel methods require a temperature of at least 75 °C [18]. Amorphous TiO_2 can be produced with the sol–gel method without the aid of heat treatment, and therefore requires less sophisticated equipment. This can help maintain low cost while providing high output, therefore increasing accessibility for adoption and in-field usage. The combination of three properties of amorphous TiO_2 provide a benefit in oil/water separation—hydrophilicity, oleophobicity, and photocatalytic activity [8,19,20]. Hydrophilicity refers to the tendency of a substance to interact with a polar solvent, in particular water. The hydrophilicity of a surface is its ability to attract water and allow wetting on it [21]. Conversely, oleophobicity is a property that describes a surface's repulsion to oils. An oleophobic surface will resist the adhesion of nonpolar liquids. Crude oil, being mostly composed of hydrocarbons, is a nonpolar liquid [22,23]. In practical use, a hydrophilic- and oleophobic-coated filter can be wetted by water while the oil collects on the surface.

To apply the self-cleaning coatings, the established sol–gel procedure was utilized to produce a titania gel that was subsequently treated and applied to fabric filters. Sol–gel treatment methods have been used to produce TiO_2 coatings. In the following experiments, the methods employed to enhance the sol–gel process are microwave radiation, refrigeration, and sonication-assisted methods.

A few studies have shown the potential of this treatment method in synthesizing and as a post-treating process [24,25]. Notably, Imoisili et al. analyzed the effect of microwave-assisted sol–gel synthesis of TiO_2. The resulting study found that microwave radiation enhances the reaction rate of forming TiO_2 nanoparticles and improves photocatalytic performance [24]. Additionally, Falk et al. concluded that microwave-assisted synthesis of TiO_2 could be obtained energy-efficiently [25]. The microwave process has also been studied to improve TiO_2 crystallization speed [26]. However, these studies either focus on increasing the reaction rate of TiO_2 formation or the enhancement of photocatalytic properties. Meanwhile, a study on the effectiveness of microwave-assisted treatment on TiO_2 coating filters is still lacking. In this work, the performance of this treatment method is investigated and compared with other treatment methods.

Hosseini et al. evaluated the effects of various treatment methods to the conventional sol–gel TiO_2 preparation [17]. The refrigeration method has been stated to produce a smaller nanoparticle size compared to microwave radiation. This method utilizes low temperature treatment to create smaller nanoparticle sizes compared to high temperature treatments. A smaller crystalline size would have a higher surface area to volume ratio. Therefore, the refrigeration treatment method would result in a better adsorption of TiO_2 on the substrate surface than a non-treated sol–gel method [17]. There are only a few studies of refrigeration treatment method for improving TiO_2 properties [17], and none of these studies had a focus on the application of TiO_2 on oil/water separation. For that reason, this paper aims to investigate the effectiveness and efficiency of this treatment method, along with others, to create a TiO_2-coated filter for oil/seawater separation.

Guo et al. demonstrated that by using the sonication method of synthesizing nanoparticle TiO_2 the nanoparticle size could be controlled between 4–5 nm, and that the methodology was "fast, simple, effective, and energy efficient" [27]. The sonication method has physical and chemical effects on the synthesis of the TiO_2 due to the cavitation phenomena that occur, which can achieve extremely high temperatures (>5000 K), pressures (>20 MPa), and cooling rates (>1010 K s^{-1}) in very localized areas that assist in the reduction of metal ions to metal or metal oxide nanoparticles [27]. Noman et al. showed that the sonication methodology could be used to produce anatase TiO_2 nanoparticles on cellulose substrate that were highly photocatalytic and possessed self-cleaning abilities [28]. Hence, the sonication-assisted sol–gel preparation method shows promise for its simplicity and energy efficiency, as well as for its ability to create small nano-particle size and selectivity towards anatase crystalline structure.

Sonication was used as a treatment method with the goal of synthesizing nanocrystalline TiO_2 with a higher ratio of the anatase crystalline structure [28]. This simple and energy efficient technique has been shown to have effective photocatalytic properties, as well as improved adhesion to fabric substrates at low temperatures [29].

A contact angle measures the interaction between a droplet and a surface. This angle quantifies the surface tension using Young's Equation [30]. Wettability also identifies the ability of a liquid to maintain contact with a surface due to the surface tension of the liquid and the interface between the liquid and a surface [16,30].

A high contact angle has a low wettability, resulting in a droplet that does not spread out across the surface. With a low contact angle, the droplet will adhere to a surface due to a higher wettability [31,32]. A high contact angle of an oil droplet on the surface of a filter is representative of low wettability to nonpolar liquids, meaning oil would be retained on the surface of the coated filter. Conversely, a low contact angle of a water droplet on the filter's surface means high wettability, generally allowing water and other polar liquids to pass through.

We propose three treatment methods to enhance the oleophobic, hydrophilic, and photocatalytic properties. Each method provides different potential benefits and provides versatility in coating production, providing flexibility when considering production facilities and material cost. Additionally, the substrates are composed of inexpensive, commonly available materials. To evaluate the filters, both substrate materials will undergo each treatment method to assess the combinations of substrate and filters, and their ability to provide effective filtration, high oil contact angle, and sufficient photo-catalytic activity. A demonstration of the oil/water separation performance of the coated filter versus an uncoated filter is provided as Video S1 in the supplementary materials.

2. Materials and Methods

2.1. Materials and Equipment

The following materials were involved in sol–gel synthesis: acetic acid glacial 99% ACS Grade (Lab Alley, Austin, TX, USA), titanium (IV), isopropoxide, TTIP (Sigma Aldrich, St. Louis, MO, USA), and 1-butanol (Sigma Aldrich). The following materials were used as substrates for titania coating: undyed cotton cloth, paper coffee filters. The following materials were used for treatment after immersing the substrates into the sol–gel: variable-wattage microwave (Sharp, Tokyo, Japan), ultrasonic bath (Branson, Brookfield, CT, USA), and 58 W refrigerator (Whirlpool, Benton Harbor, MI, USA).

2.2. Coated Filter Preparation

The sol–gel method is simple and one of the most effective methods for producing nano-sized metallic oxide materials [33]. To reduce the reactivity of the alkoxide and stabilize the solution, TTIP was gradually dissolved in 1-butanol at room temperature with magnetic stirring. 1-butanol was chosen because it can synthesize the smallest nanoparticle size in sol–gel method among different alcohol solvents [34]. The acetic acid was then added dropwise with magnetic stirring for 120 min. The reactants were introduced gradually, as this is an exothermic reaction.

2.2.1. Refrigeration-Assisted Treatment

The filter was completely immersed in the sol–gel container. The container was stored without covering in a refrigerator at 4 °C for 24 h. The coated filter was allowed to dry at room temperature for 24 h.

2.2.2. Microwave-Assisted Treatment

The substrate was completely immersed in room temperature sol–gel and placed into a microwave equipment. The solution, immersed in a sol–gel bath, was irradiated by microwaves at 1500 W in two 20 s intervals to prevent the solution from boiling over, with 40 s between the intervals to cool. By calculation, the total input energy for irradiation was 60 kJ. However, this amount of input energy may not completely contribute to the sol–gel treatment due to the volume effect and other parts being heated. After the microwave treatment, the substrate was left to cool and dry in a well-ventilated area at room temperature for 24 h.

2.2.3. Sonication-Assisted Treatment

During the sonication treatment method, the sol–gel mixture was immersed in a sonication bath and sonicated for a total time period of 10 min, with the ultrasonicator power level set at 100 W. The energy input was calculated for sonication to be 60 kJ. This sonicated solution was then used to coat the substrates. After immersing the substrates in the solution for 24 h, they were allowed to dry at room temperature for 24 h.

2.3. Porosity Ratio

The relative porosity between the cloth and coffee control was determined as a ratio. Two sample strips from the control filters with the same dimension were prepared. Each

strip was fully immersed in hexane for 20 s and removed afterward. The mass difference of the hexane between prior and after the immersion was recorded. The porosity ratio could be calculated using the following equation:

$$\frac{\phi_{\text{coffee filter}}}{\phi_{\text{cotton}}} = \frac{V_{\text{pore,coffee}}}{V_{\text{pore,cotton}}}\left(\frac{V_{\text{cotton sample}}}{V_{\text{coffee sample}}}\right) = \frac{m_{\text{soaked hexane,coffee}}}{m_{\text{soaked hexane,cotton}}}\left(\frac{\delta_{\text{cotton}}}{\delta_{\text{coffee}}}\right) \approx \frac{m_{\text{soaked hexane,coffee}}}{m_{\text{soaked hexane,cotton}}} \quad (1)$$

where ϕ is the porosity, m is the mass of the soaked hexane in the coffee or cloth control sample, and δ is the thickness of the material. Since the thickness is much smaller than the surface area of the samples, the volume ratio of the sample can be approximate to the surface area ratio, which was controlled to be 1. Therefore, the porosity ratio between the cloth and coffee filter material could be determined as the mass ratio of the mass difference of the hexane.

2.4. Mass Distribution

The mass distribution of TiO_2 on different coated filters was measured as mass per unit surface area. Six square pieces of substrate samples, 3 from cloth and 3 from coffee filter, were measured and prepared to have the same dimensions. These pre-weighed samples were TiO_2 coated with different treatment methods. After the coating and drying process, the samples were reweighed. The mass distribution of TiO_2 would be the mass difference between prior and after the coating process over the surface area of the substrate.

$$\text{Mass distribution} = \frac{\text{Mass difference}}{\text{Surface area of substrate}} \quad (2)$$

2.5. Performance Testing

Two tests were conducted to evaluate the performance of each type of coated filter, including the filtration test and static contact angle test. In the filtration test, a funnel with the tested filter was set atop a graduated cylinder. In the contact angle test, a UHD resolution camera with Xenvo Clarus 15x Macro Lens attachment was used to capture the images of the droplets on a flat filter surface. The contact angles were determined using image-analyzing software.

2.5.1. Pure Oil Filtration Test

A timed gravity filtration test with pure oil was conducted to obtain quantifiable values of the filtration capabilities between the coated against their respective control filters, and between the various treatment methods in comparison to one another [35,36].

The test was conducted by pouring 50 mL of pure motor oil onto the filter contained within a funnel, which was then allowed to gravity filtrate over a period of 5 min. The funnel was set atop a 50 mL graduated cylinder. During the duration of the test, the filtrate volume was recorded in 30 s intervals.

To analyze the increased filtration performance, the data from the filtration test are represented as a percentage improvement of the coated filter against the control filter. This is calculated as the additional volume of oil that the coated filter blocked from passing, divided by the original volume of oil that passed through the control filter.

$$\%\ \text{Improvement} = \frac{V_{\text{filtrate,control}} - V_{\text{filtrate,coated}}}{V_{\text{filtrate,control}}} \times 100\% \quad (3)$$

2.5.2. Contact Angle Test

Contact angle was used to measure the oleophobic qualities of the filter where a higher contact angle will be seen with filter with higher oleophobicity [37]. It was predicted that the treated filter would have a higher contact angle compared to the untreated filter.

To measure the contact angle of the filter, a video was taken of a 25 mm^3 droplet of motor oil (ProLine SAE 10W40) being dropped onto the filter. A single image was taken

from the video when the droplet first made contact and was observed with the use of software add-ons (Drop Shape Analysis and Contact Angle) to ImageJ (Version 1.53k, U.S. National Institutes of Health, Bethesda, MD, USA) to determine the contact angle, as shown in Figure 1. The averages of both contact angle analysis software were averaged to provide the contact angle.

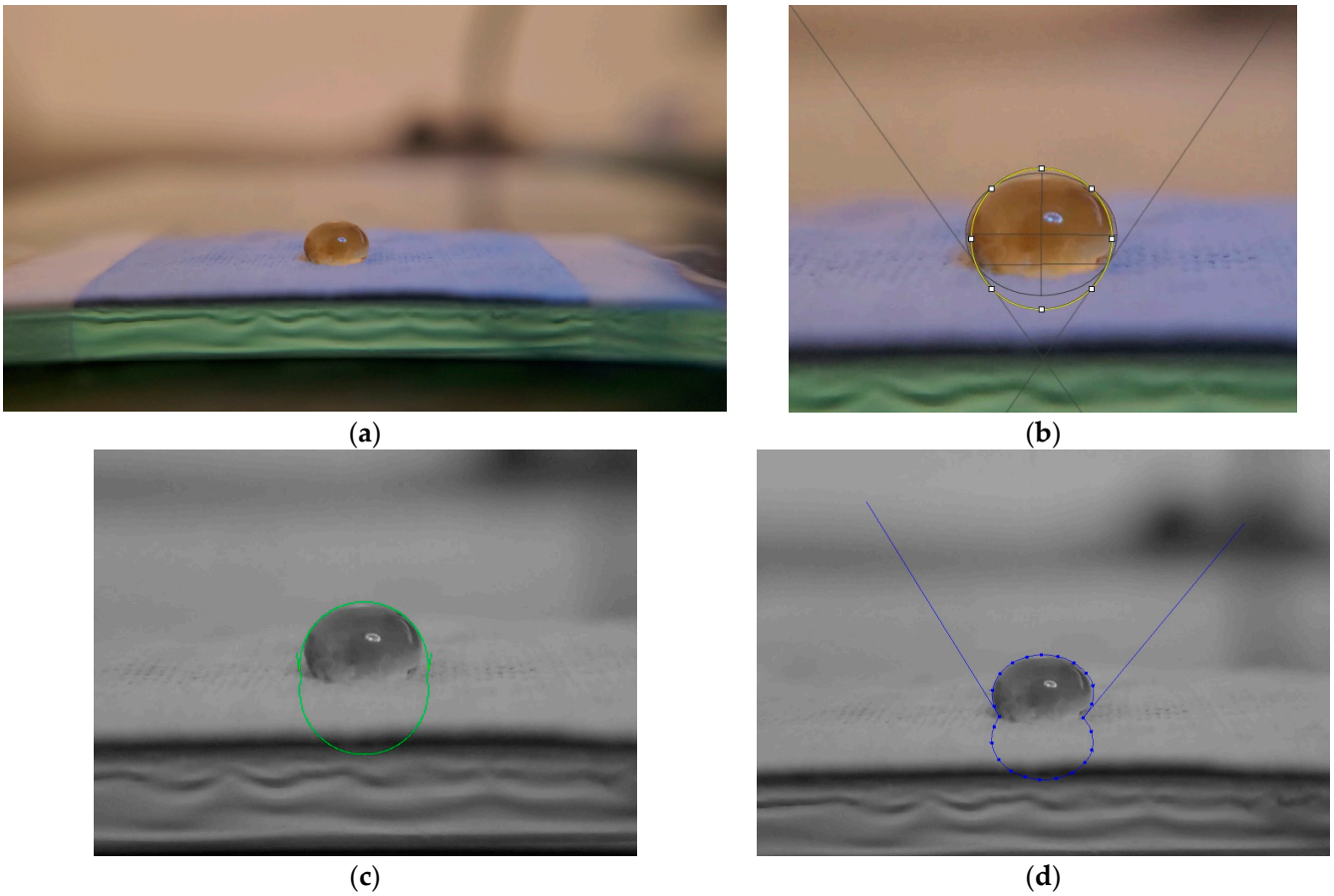

Figure 1. (**a**) Oil droplet on filter; (**b**) Droplet observed using ImageJ Contact Angle Plugin; (**c**) ImageJ Drop Shape Analysis Plugin (LB-ADSA); (**d**) ImageJ Drop Shape Analysis Plugin (DropSnake).

2.5.3. Photocatalytic Activity Assessment

To confirm the coated filter's ability to undergo photocatalysis, the reagent methylene blue (MB) was applied onto the filters and exposed to sunlight over a total period of 20 h of sunlight as shown in Figure 2. Titania's property to decompose organic substances under sunlight UV irradiation will cause the MB to fade in color [38]. Photos were taken in increments of 10 h to qualitatively assess the color degradation during the duration of their exposure.

A color grading software add-on (Color Histogram) for ImageJ was used to analyze and numerically evaluate the color degradation of MB on the coated filters. A reference Red Green Blue (RGB) value was recorded for each treatment method and substrate type. The RGB value of the filters was also recorded immediately upon being stained with MB. As the MB decomposed on the filter surface due to sunlight exposure, the RGB value approaches its control value, providing a quantitative measurement of coating photocatalysis. The RGB values were evaluated as the percentage similarity to the reference RGB value. A higher percentage difference represents greater photocatalytic degradation ability, expressed by the TiO_2 coating.

$$\%\ \text{RGB Similarity} = \left(1 - \frac{\text{RGB}_{\text{ref.}} - \text{RGB(t)}}{\text{RGB}_{\text{ref.}}}\right) \times 100\% \quad (4)$$

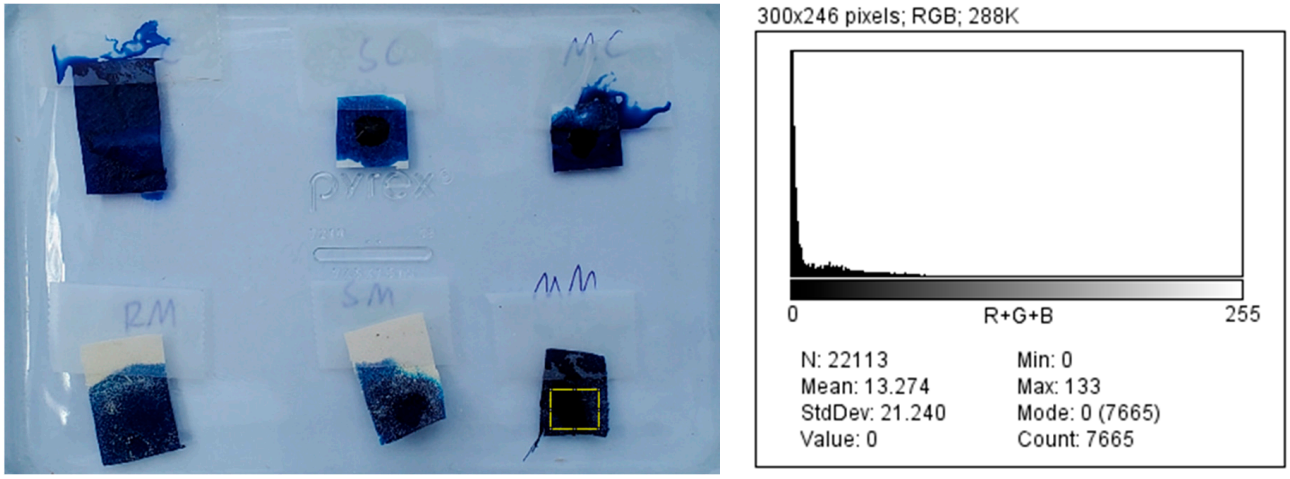

(**a**) (**b**)

Figure 2. (**a**) Filters soaked in methylene blue; (**b**) Color histogram using ImageJ.

2.6. Characterization

X-ray crystallography was used to identify the composition of the resulting products of sol–gel synthesis and treatment. To prepare the samples for x-ray diffraction (XRD), the liquid samples of treated sol–gel were allowed to dry in enclosed area with a silica gel desiccant. The resulting dried particles were examined using a Bruker D2 PHASER.

3. Results and Discussion

3.1. Oil Filtration and Oil–Water Separation Efficiency

Figure 3 shows the data collected from the gravity filtration test. Smaller volumes of oil filtrate represent better filtration performance, as it is more effective at separating the oil from the water. The filtration test results demonstrated that all treatment methods showed an improvement in filtration capabilities versus their respective uncoated control filters.

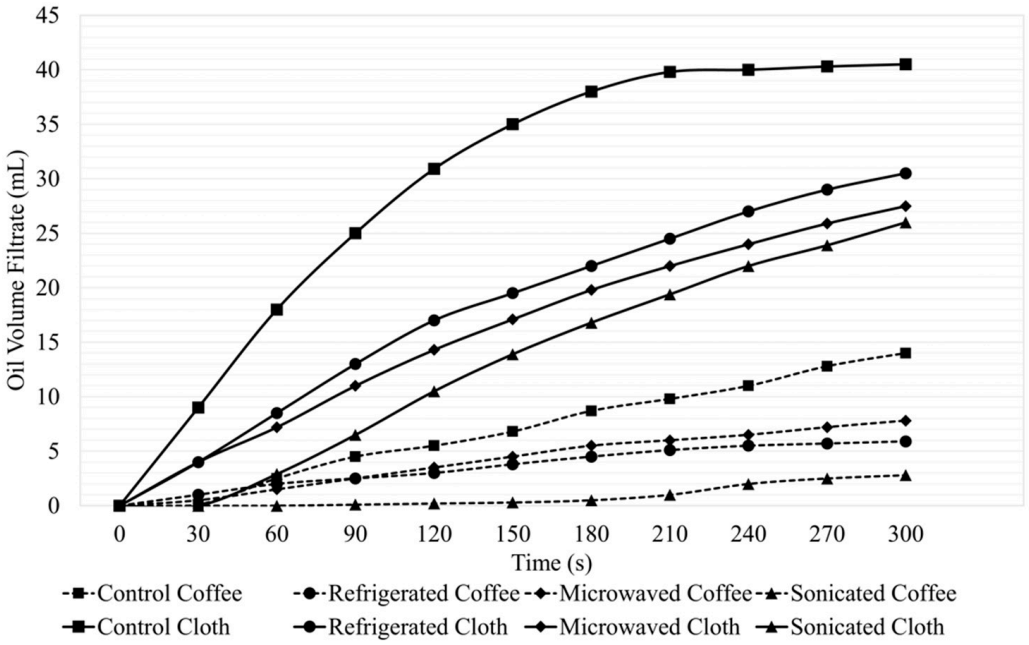

Figure 3. Volume of oil filtrate as a function of time.

The results in Figure 4 were presented as percentage improvements against their control filters. The coated coffee filters have shown a greater enhancement compared to the

cloth filters across all treatment methods. Sonication treatment proved to have the highest improvement factor, with sonicated coffee filters having an 80% increase and cloth filters showing a 36% improvement.

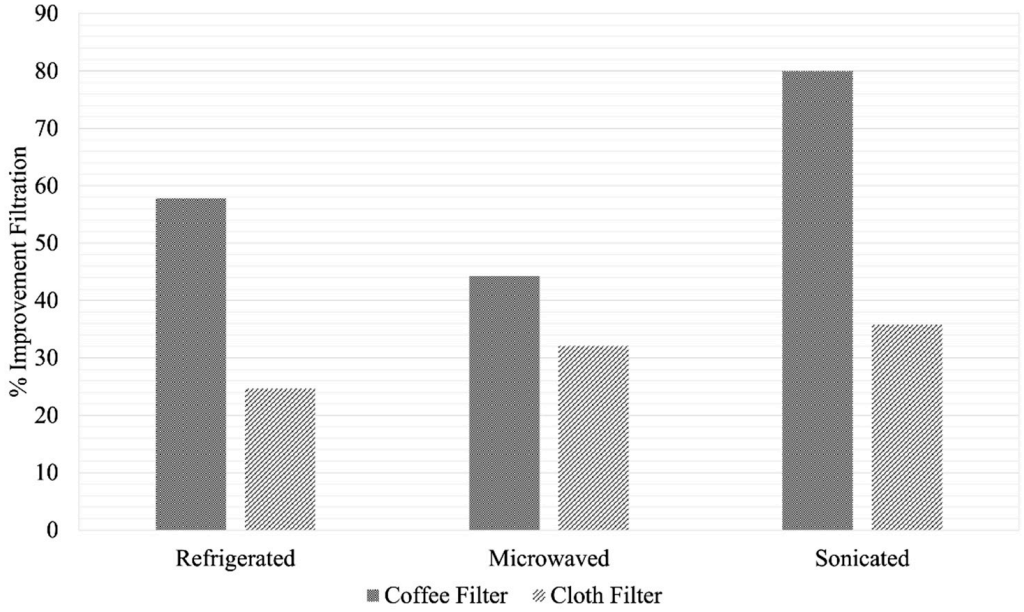

Figure 4. Percent improvement on filtration efficiency of the filter made under different treatment methods.

Another gravity-timed filtration test was done for oil and simulated seawater. However, the test results provide valuable data for this work. Because of the opposite characteristics in polarity, oil and seawater are not soluble in each other, causing a water barrier layer for oil to not pass through the filter and vice versa. As a result, there would be little or no amount of filtrate passed in a short period of testing time. The coated filters were also confirmed to not be hydrophobic with a simulated seawater filtration test. Therefore, for the timed filtration test of oil/simulated seawater, the results were not valid in determining the efficiency of separation. This reinforces the purpose of the oil filtration test to investigate the oleophobicity of the filter to evaluate filtration efficiency.

3.2. Wettability of Oil to Different Oil Filters

Figure 5 depicts a data analysis of the static contact angle. In comparison to the control filters, all treated filters had a greater oil contact angle, which indicated that the TiO_2 coating increased the oleophobicity of the filters. However, the treatment methods did not show any correlation with the contact angles. The microwaved filter had the highest contact angle among cotton filters. On the other hand, it had the lowest contact angle among coated coffee filters. The amount by which the contact angle rose varied depending on the treatment procedure and filter type. In cloth filters, sonication and microwave treatment methods raised the contact angle considerably more than refrigeration. The control cloth filter had a greater oil contact angle than the control coffee filter. This was maintained after coating, as coated cloth filters had consistently higher contact angles that coated coffee filters. This suggests that treatment temperature has a significant effect on filter oleophobicity and should be taken into consideration when choosing substrate material and treatment type. In future work, the oleophobicity of the filters should be expanded upon via testing using the Washburn method via a force tensiometer.

All filters were also tested with water to confirm that they retained the hydrophilic properties of the control filters. Droplets were absorbed into the filter too rapidly to determine a contact angle, suggesting extremely high hydrophilicity.

Despite their greater filtration performance, ultrasonicated filters do not have a considerably larger contact angle. This could be due to the distribution of TiO_2 particles on

the filter. Ungan and Tekin (2019) [39] showed that sonication of sol–gel solution evenly distributes TiO_2 particles. This could result in filters immersed in the sonicated sol–gels having higher average coating density per area.

Additionally, a larger substrate pore radius leaves less surface area for TiO_2 to adhere to upon sol–gel immersion. From Table 1, the pore ratio between coffee versus cloth filters was determined to be 0.25, meaning cloth filters have a larger pore size. Therefore, cloth was shown to have greater permeability due to its higher pore size [40]. This is also demonstrated by control cloth filters allowing a higher volume of oil filtrate than control coffee filters in the filtration test. As a result, porous substrates provide less effective coated filters.

Another potential explanation for the inconsistent performance of filters between filtration and contact angle test could include droplet volume variation and the limitations of the imaging software. Droplet volume typically does not have a significant impact on contact angle within the microliter scale on ideal surfaces, as Drelich (2006) describes ideal surfaces as having a smooth surface and homogeneity [41]. The fabric filters used in experimentation have rough and uneven surfaces. This may increase the effect of droplet volume on the measured contact angle. Furthermore, when the droplet volume increases, the effect of gravity also increases [42], which could result in an inaccurate contact angle comparison.

Figure 6 presents the TiO_2 mass distribution on different coated filters. On the same type of substrate, all treatment methods deposited the same amount of TiO_2 coating. Between the two substrate types, cloth filters had a considerably higher mass of TiO_2. This could be explained by the higher porosity of cloth substrates, leaving more vacancies for the TiO_2 particles to be deposited on the surface. Moreover, a consistent distribution of TiO_2 between different treatment methods suggest that the coating is distributed evenly. However, scanning electron microscope (SEM) imaging is required to confirm the evenness of the coating.

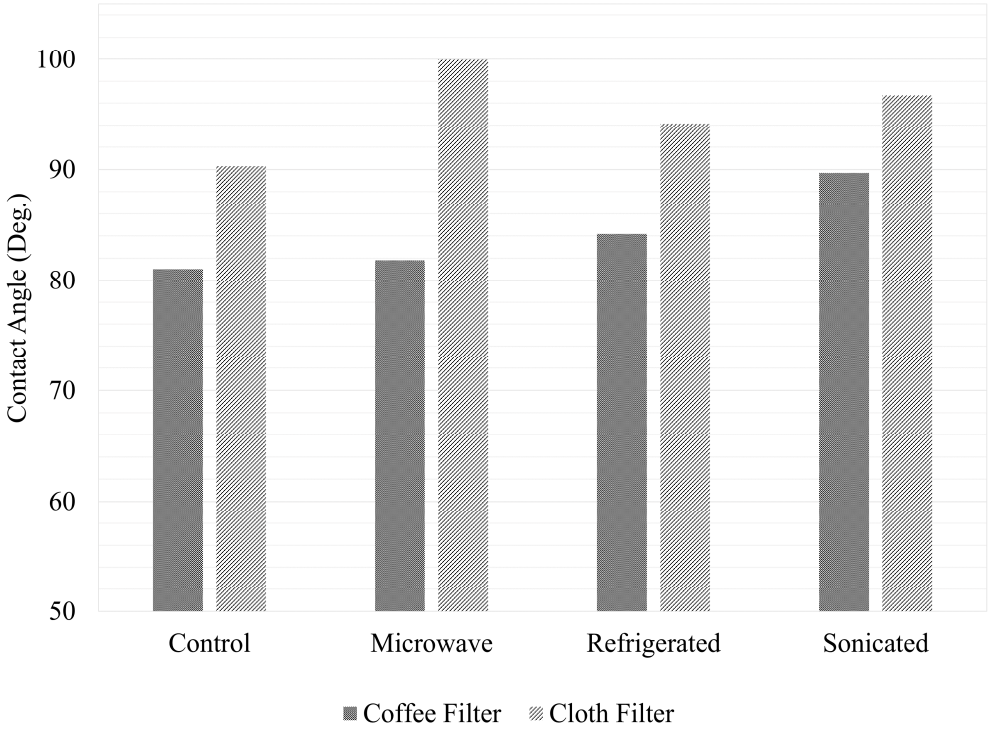

Figure 5. Contact angle of filters treated by different methods.

Table 1. Porosity Ratio of Coffee Filter and Cloth Substrate.

	Coffee Filter	Cloth
Mass of soaked hexane (g)	0.20	0.80
Porosity ratio ($\varphi_{coffee}/\varphi_{cloth}$)	0.25	

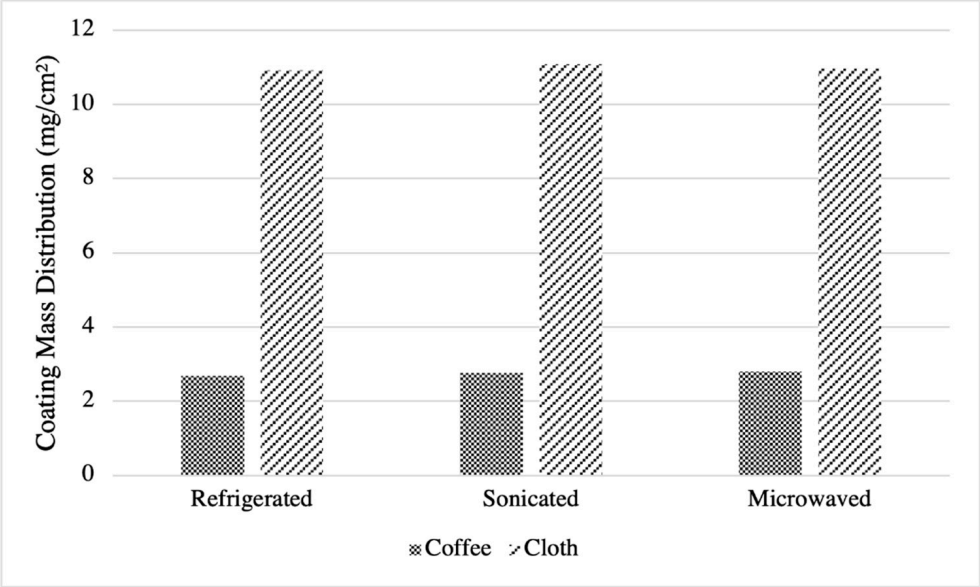

Figure 6. Mass distribution of TiO_2 on filters with different treatment methods.

3.3. Photocatalytic Decomposition of Dye by the Coated Filters

Figure 7 shows the color degradation of methylene blue dye on multiple coated filters. After 20 h of exposure to sunlight, the filter for all treatment types and substrate material had visibly discolored. This confirms TiO_2 coated filter's ability to degrade organic compounds in the presence of ultraviolet light.

In Figure 8, the RGB similarity explained by Equation 2 uses the un-dyed filter as the reference. Based on the results, the refrigerated cloth was the best at returning to its original state. The refrigerated cloth filter returned to 55% of its original RGB value after 20 h of sun exposure. Both microwaved filters, however, performed the worst during the test. Therefore, microwave treatment is not the ideal choice when photocatalytic ability is of high priority.

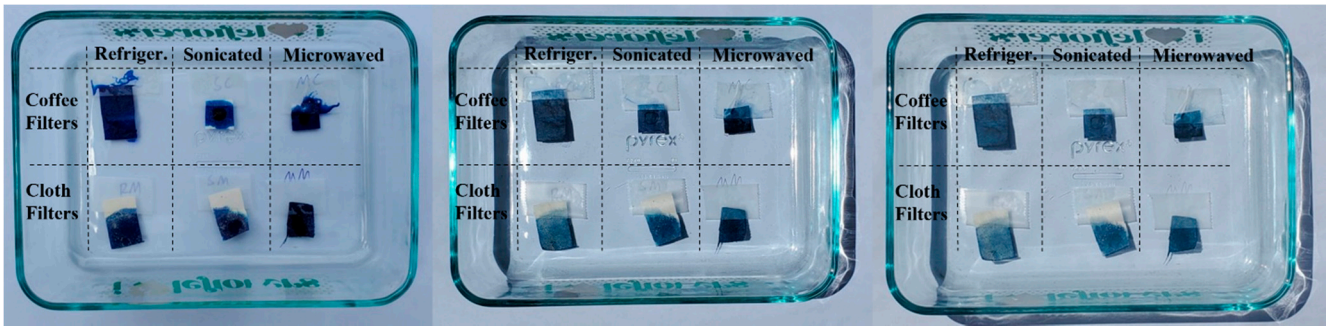

Figure 7. Color degradation results from left to right: after 0, 10, and 20 h. Organized into a table by substrate material (vertical axis) and treatment types (horizontal axis).

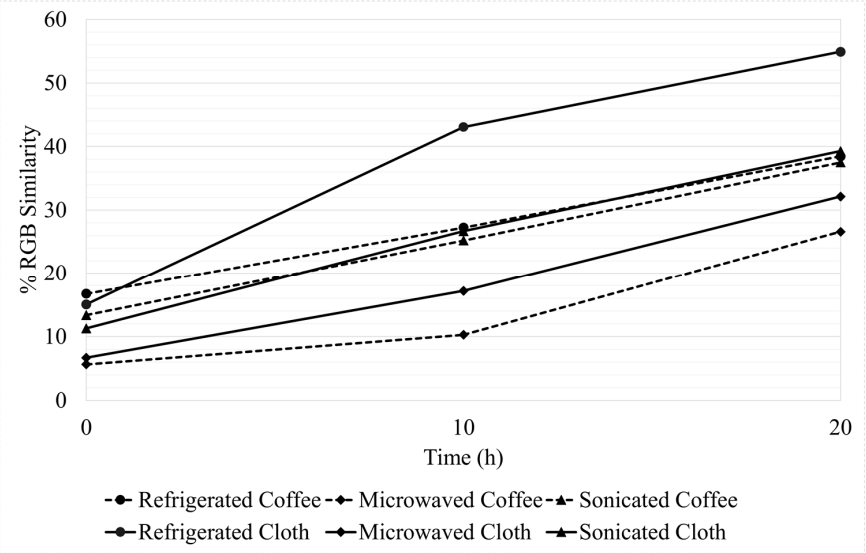

Figure 8. Percent RGB similarity as a function of time.

3.4. Structure of the Oxide Coating Determined by XRD

XRD was used on another batch of sol–gel, synthesized for the purpose of examining the phase of TiO_2. This batch of sol–gel was treated in the same manner as those used in the previous trials. The sol–gel samples of all treatment methods were found to contain amorphous phase TiO_2. The additional compounds used in synthesizing the sol–gel, 1-Butanol, and acetic acid are volatile liquids and were allowed to completely vaporize over a span of 14 days. Therefore, they are not present in the samples.

The XRD results shown in Figure 9 do confirm the presence of amorphous TiO_2 with no presence of any crystalline forms of TiO_2. Despite the lack of anatase phase crystals, the amorphous coating was able to provide favorable oil/water separation properties. This result is promising for scalable production of filters, as amorphous TiO_2 can be formed without requiring additional heat treatment or as much highly sophisticated equipment. If the amorphous coating is able to be further optimized, it is more likely to be implemented in oil spill cleanup efforts.

3.5. Reaction Mechanisms for Sol–Gel Coating Formation and Photocatalysis

The formation of the sol–gel coating may be divided into several steps. In the first step, the TTIP hydrolysis generated titanium hydroxide. The reaction can be expressed by:

$$TTIP + H_2O \rightarrow Ti(OH)_4 + CH_3CH_2OH$$

After the sol–gel formation, we carried out the immersion of the filter materials, including cloth cotton and coffee filter paper, which were soaked with the titanium hydroxide sol and gel. The next step of drying allowed the amorphous titanium dioxide generation:

$$Ti(OH)_4 \rightarrow TiO_2 + 2H_2O$$

As a nanoparticle coating on the filter materials, the titanium oxide showed photoactivity because of the electron and hole rejection:

$$TiO_2 + h_\nu \rightarrow TiO_2 + e^- + h^+$$

The electron ejection helps the interaction with the polar solvent water. That is why the increased hydrophilicity was observed after the coating was applied. The positive changed hole allowed the reaction of organics decomposition, as can be expressed by:

$$R + h^+ \rightarrow R1 + R2$$

where R, R1, and R2 are carbon chain compounds with different carbon chain length. R is a long chain compound, while R1 and R2 have shorter chain lengths.

The existence of the hole caused the chain broken of dye or oil and eventually may convert them into low molecular compounds by releasing carbon dioxide simultaneously [14].

For future works, we look towards other approaches to enhance oil/water separation. Additional types of filter substrates beside natural fibers should be tested, in addition to different surface modifications. For example, Nowak et al. used a polypropylene substrate modified with MTMS aerogel for oil aerosol separation [43]. A polypropylene substrate could potentially provide significant oil/water separation benefits while maintaining low cost. Additionally, Nowak et al. described the addition of multiple layers of filters, which could increase the overall efficiency of the filtration process. An additional study on the potential of the service lifetime and reusability of the filter would be beneficial.

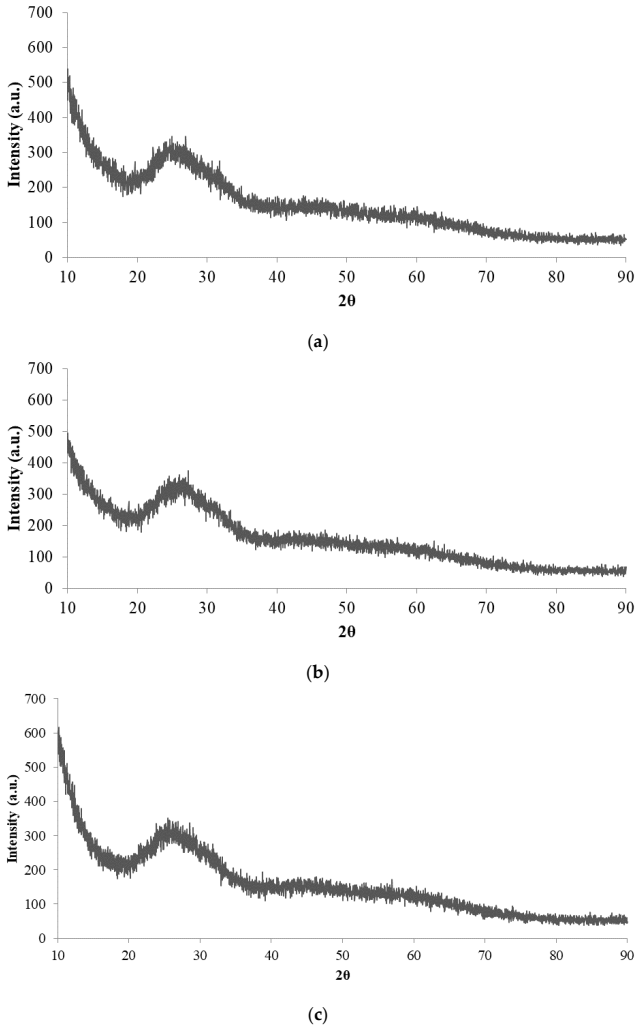

Figure 9. XRD results for (**a**) microwaved, (**b**) refrigerated, and (**c**) sonicated TiO_2 (from top to bottom order).

4. Conclusions

The sol–gel method used in this study successfully created and deposited TiO_2 on both the natural fiber substrates used during experimentation. All coating treatment methods increased the filters' oil/water filtration capability, resisting the passage of oil. Additionally, all coatings increase the filters' oil contact angle, indicating an increase in their oleophobicity. Of the tested treatment methods, sonication treatment had the most significant increase during filtration test, with an improvement of 80%. Coffee filters had better filtration performance, suggesting that smaller pore size may give more surface area for TiO_2 to adhere to the filters.

Testing with methylene blue showed that all the filters were imparted with photocatalytic properties from the TiO_2 coating. XRD analysis on samples of treated sol–gel showed the main phase of the coatings to be amorphous. Increasing the treatment durations may lead to more anatase phase formation. Overall, our experimentation produced promising results towards the synthesis of a highly reproducible filter for oil cleanup efforts.

Future experiments should perform further analysis on additional substrate materials, substrate pre-treatment, sol–gel treatment duration, and better filter curing conditions to further improve filtration capability. Additional studies on the effect of treatment method on TiO_2 phase, as well as further evaluation to provide quantitative data on the photocatalytic properties on different substrates, could be conducted.

Supplementary Materials: The following supporting information can be downloaded at: https://www.mdpi.com/article/10.3390/separations9100269/s1. Video S1: Oil Water Separation by Titania Coating.

Author Contributions: Conceptualization, M.L. and H.R.; methodology, H.R., H.N. and B.N.; software, H.R. and B.N.; validation, M.L.; formal analysis, H.R., H.N., B.N. and A.F.; investigation, H.R., H.N., B.N., A.F., J.S. and M.P.; resources, M.L. and H.R.; data curation, H.R.; writing—original draft preparation, H.R., H.N., B.N., A.F., J.S. and M.P.; writing—review and editing, M.L. and Y.X.G.; visualization, H.R., H.N., B.N. and A.F.; supervision, M.L. and Y.X.G.; project administration, M.L. All authors have read and agreed to the published version of the manuscript.

Funding: This research received no external funding.

Institutional Review Board Statement: Not applicable.

Informed Consent Statement: Not applicable.

Data Availability Statement: Data is contained within the article and Supplementary Materials.

Acknowledgments: The authors would like to thank Noor Halabi, and An Nguyen for their assistance in gathering contact angle data, Harjot Singh, and Vilupanur Ravi for their assistance with XRD.

Conflicts of Interest: The authors declare no conflict of interest. No funders were involved in the design of the study in the collection, analyses, or interpretation, of data; in the writing of the manuscript, or in the decision to publish the results.

References

1. Huntington Beach 2022 Water Quality Report. City of Huntington Beach, California. Available online: https://huntingtonbeachca.gov/files/users/public_works/2022-Drinking-Water-Quality-Report.pdf (accessed on 16 August 2022).
2. Office of Emergency and Remedial Response, Agency Response PB2000-963401 Oil Program Center Understanding Oil. United States Environmental Protection Agency. Available online: https://www.epa.gov/sites/default/files/2018-01/documents/ospguide99.pdf (accessed on 16 August 2022).
3. Office of Response and Restoration. How Do Oil Spills out at Sea Typically Get Cleaned Up? National Oceanic and Atmospheric Administration. Available online: https://response.restoration.noaa.gov/about/media/how-do-oil-spills-out-sea-typically-get-cleaned.html (accessed on 15 August 2022).
4. Nakajima, A.; Koizumi, S.I.; Watanabe, T.; Hashimoto, K. Photoinduced amphiphilic surface on polycrystalline anatase TiO_2 thin films. *Langmuir* **2000**, *16*, 7048–7050. [CrossRef]
5. Wang, Y.; Gong, X. Special oleophobic and hydrophilic surfaces: Approaches, mechanisms, and applications. *J. Mater. Chem. A* **2017**, *5*, 3759–3773. [CrossRef]

6. Li, S.; Huang, J.; Ge, M.; Cao, C.; Deng, S.; Zhang, S.; Chen, G.; Zhang, K.; Al-Salem, S.; Lai, Y. Robust flower-like TiO_2@Cotton fabrics with special wettability for effective self-cleaning and versatile oil/water separation. *Adv. Mater. Interfaces* **2015**, *2*, 1500220. [CrossRef]
7. Shi, H.; He, Y.; Pan, Y.; Di, H.; Zeng, G.; Zhang, L.; Zhang, C. A modified mussel-inspired method to fabricate TiO_2 decorated superhydrophilic PVDF membrane for oil/water separation. *J. Membr. Sci.* **2016**, *506*, 60–70. [CrossRef]
8. Li, F.; Kong, W.; Zhao, X.; Pan, Y. Multifunctional TiO_2-based superoleophobic/superhydrophilic coating for oil–water separation and oil purification. *ACS Appl. Mater. Interfaces* **2020**, *12*, 18074–18083. [CrossRef]
9. Gao, C.; Sun, Z.; Li, K.; Chen, Y.; Cao, Y.; Zhang, S.; Feng, L. Integrated oil separation and water purification by a double-layer TiO_2-based mesh. *Energy Environ. Sci.* **2013**, *6*, 1147–1151. [CrossRef]
10. Banerjee, S.; Dionysiou, D.D.; Pillai, S.C. Self-cleaning applications of TiO_2 by photo-induced hydrophilicity and photocatalysis. *Appl. Catalysis B Environ.* **2015**, *176*, 396–428. [CrossRef]
11. Li, T.; Dong, C.; Liu, Y.; Wu, J.; Zhang, X.; Gong, X.; Zhao, W.; Wang, D.; Zhu, D. An anodized titanium/sol-gel composite coating with self-healable superhydrophobic and oleophobic property. *Front. Mater.* **2021**, *8*, 618674. [CrossRef]
12. Wise, J.; Wise, J.P., Sr. A review of the toxicity of chemical dispersants. *Rev. Envir. Health* **2011**, *26*, 281–300. [CrossRef]
13. Faksness, L.G.; Leirvik, F.; Taban, I.C.; Engen, F.; Jensen, H.V.; Holbu, J.W.; Dolva, H.; Bratveit, M. Offshore filed experiments with in-situ burning of oil: Emissions and burn efficiency. *Environ. Res.* **2022**, *205*, 112419. [CrossRef]
14. Schneider, J.; Matsuoka, M.; Takeuchi, M.; Zhang, J.; Horiuchi, Y.; Anpo, M.; Bahnemann, D.W. Understanding TiO_2 Photocatalysis: Mechanisms and Materials. *Chem. Rev.* **2014**, *114*, 9925–9933. [CrossRef] [PubMed]
15. Pelaez, M.; Nolan, N.T.; Pillai, S.C.; Seery, M.K.; Falaras, P.; Kontos, A.G.; Dunlop, P.S.M.; Hamilton, J.W.J.; Byrne, J.A.; O'Shea, K.; et al. A review on the visible light active titanium dioxide photocatalysis for environmental applications. *Appl. Catal. B Environ.* **2012**, *125*, 332–334. [CrossRef]
16. Vrakatseli, V.; Farsari, E.; Mataras, D. Wetting properties of transparent anatase/rutile mixed phase glancing angle magnetron sputtered nano-TiO_2 films. *Micromachines* **2020**, *11*, 616. [CrossRef] [PubMed]
17. Hosseini, M.S.; Sadeghi, M.T. Improving oleophobicity and hydrophilicity of superhydrophobic surface by TiO_2-based coatings. *Mater. Res. Express* **2018**, *5*, 085010. [CrossRef]
18. Ao, Y.; Xu, J.; Fu, D.; Shen, X.; Yuan, C. Low temperature preparation of anatase TiO_2-coated activated carbon. *Colloids Surf. A Physicochem. Eng. Asp.* **2007**, *312*, 125–127. [CrossRef]
19. Sun, S.; Song, P.; Cui, J.; Liang, S. Amorphous TiO_2 nanostructures: Synthesis, fundamental properties and photocatalytic applications. *Catal. Sci. Technol.* **2019**, *16*, 6–12. [CrossRef]
20. Kameya, Y.; Yabe, H. Optical and Superhydrophilic Characteristics of TiO_2 Coating with Subwavelength Surface Structure Consisting of Spherical Nanoparticle Aggregates. *Coatings* **2019**, *9*, 547. [CrossRef]
21. Muller, P. Glossary of terms used in physical organic chemistry (IUPAC Recommendations 1994). *Pure Appl. Chem.* **1994**, *66*, 1077–1184. [CrossRef]
22. Altawell, N. Financing for rural electrification. In Proceedings of the IEEE Conference on Computational Intelligence for Financial Engineering & Economics, New York, NY, USA, 29–30 March 2012.
23. McKeen, L.W. *Film Properties of Plastics and Elastomers*, 4th ed.; William, A., Ed.; Elsevier: Amsterdam, The Netherlands, 2017; pp. 1–23.
24. Imoisili, P.E.; Jen, T.C.; Safaei, B. Microwave-assisted sol–gel synthesis of TiO_2-mixed metal oxide nanocatalyst for degradation of organic pollutant. *Nanotechnol. Rev.* **2021**, *10*, 126–136. [CrossRef]
25. Padrisi, E.; Rosa, R.; Baldi, G.; Dami, V.; Cioni, A.; Lorenzi, G.; Leonelli, C. Microwave-Assisted Vacuum Synthesis of TiO_2 Nanocrystalline Powders in One-Pot, One-Step Prodedure. *Nanomaterials* **2021**, *12*, 149.
26. Tao, Y.; Wu, C.Y.; Mazyck, D.W. Microwave-Assisted Preparation of TiO_2/Activated Carbon Composite Photocatalyst for Removal of Methanol in Humid Air Stream. *Ind. Eng. Chem. Res.* **2006**, *14*, 5110–5116. [CrossRef]
27. Guo, J.; Zhu, S.; Chen, Z.; Li, Y.; Yu, Z.; Liu, Q.; Li, J.; Feng, C.; Zhang, D. Sonochemical synthesis of TiO_2 nanoparticles on graphene for use as photocatalyst. *Ultrason. Sonochemistry* **2011**, *18*, 1082–1090. [CrossRef] [PubMed]
28. Sadr, F.A.; Montazer, M. In situ sonosynthesis of nano TiO_2 on cotton fabric. *Ultrason. Sonochemistry* **2014**, *21*, 681–691. [CrossRef]
29. Lee, H.J. Improving superhydrophobic textiles materials. In *Functional Textiles for Improved Performance, Protection and Health*, 1st ed.; Pan, N., Sun, G., Eds.; Woodhead Publishing Limited: Cambridge, UK, 2011; Volume 2, pp. 339–359.
30. Moldoveanu, S.C.; David, V. RP-HPLC analytical columns. In *Selection of the HPLC Method in Chemical Analysis*; Elsevier: Boston, MA, USA, 2017; pp. 279–328.
31. Sarkar, M.; Hasanuzzaman, M.; Gulshan, F.; Rashid, A. Surface, mechanical and shape memory properties of biodegradable polymers and their applications. *Encycl. Mater. Plast. Polym.* **2022**, *2*, 1092–1099.
32. Contact Angle and Surface Tension—A Fascinating Liaison. Available online: https://www.cscscientific.com/csc-scientific-blog/how-does-contact-angle-relate-to-surface-tension#:~{}:text=A%20low%20contact%20angle%20(left,the%20quality%20of%20a%20liquid (accessed on 16 August 2022).
33. Ye, L.; Zhang, Y.; Song, C.; Li, Y.; Jiang, B. A simple sol-gel method to prepare superhydrophilic silica coatings. *Mater. Lett.* **2017**, *188*, 316–318. [CrossRef]
34. Wiranwetchayan, O.; Promnopas, S.; Thongtem, T.; Chaipanich, A.; Thongtem, S. Effect of alcohol solvents on TiO_2 films prepared by sol–gel method. *Surf. Coat. Technol.* **2017**, *326*, 310–315. [CrossRef]

35. Sadler, E.; Crick, C.R. Suction or gravity-fed oil-water separation using PDMS-coated glass filters. *Sustain. Mater. Technol.* **2021**, *29*, e00321. [CrossRef]
36. Kroeger, R.M.; DeKay, H.G. Measurement of gravity filtration. *J. Am. Pharm. Assoc.* **1951**, *40*, 213–215. [CrossRef]
37. Xue, C.H. Improving superhydrophobic coatings for textiles through chemical modifications. In *Functional Textiles for Improved Performance, Protection and Health*, 1st ed.; Pan, N., Sun, G., Eds.; Woodhead Publishing Limited: Cambridge, UK, 2011; Volume 2, pp. 320–338.
38. Yan, X.; Ohno, T.; Nishijima, K.; Abe, R.; Ohtani, B. Is methylene blue an appropriate substrate for a photocatalytic activity test? A study with visible-light responsive titania. *Chem. Phys. Lett.* **2006**, *429*, 606–610. [CrossRef]
39. Ungan, H.; Tekin, T. Effect of the sonication and coating time on the photocatalytic degradation of TiO_2, TiO_2-Ag, and TiO_2-ZnO thin film photocatalysts. *Chem. Eng. Commun.* **2020**, *207*, 896–903. [CrossRef]
40. Nishiyama, N.; Yokoyama, T. Permeability of porous media: Role of the critical pore size. *J. Geophys. Res. Solid Earth* **2017**, *122*, 6955–6971. [CrossRef]
41. Drelich, J. The effect of drop (bubble) size on contact angle at solid surfaces. *J. Adhes.* **1997**, *63*, 31–51. [CrossRef]
42. Ren, H.; Xu, S.; Wu, S.T. Effects of gravity on the shape of liquid droplets. *Opt. Commun.* **2010**, *283*, 3255–3258. [CrossRef]
43. Nowak, B.; Bonora, M.; Zuzga, M.; Werner, L.; Jackiewicz-Zagorska, A.; Gac, J.M. MTMS-based aerogel structure deposition on propylene fibrous filter—Surface layer effect and distribution control for improvement of oil aerosol separation properties. *J. Environ. Chem. Eng.* **2022**, *10*, 108410. [CrossRef]